

# 1 Improvement of FAO-56 model to estimate transpiration fluxes of 2 drought tolerant crops under soil water deficit: An application for 3 olive groves

4  
5 *G. Rallo<sup>1</sup>, G. Baiamonte<sup>2</sup>, J. Manzano Juárez<sup>3</sup> and G. Provenzano<sup>4</sup>*

6  
7 <sup>1</sup>*PhD, Junior Investigator. Dipartimento Scienze Agrarie e Forestali (SAF), Università degli*  
8 *Studi, Viale delle Scienze 12, Palermo, Italy email: rallo.giovanni@gmail.com*

9 <sup>2</sup>*PhD, Associate Professor. Dipartimento Scienze Agrarie e Forestali (SAF), Università degli*  
10 *Studi, Viale delle Scienze 12, Palermo, Italy.*

11 <sup>3</sup>*Ph.D. Researcher, Departamento de Ingeniera Rural y Agroalimentaria, Unidad Hidráulica,*  
12 *Univ. Politécnica de Valencia, Camino de vera s/n, 46022 Valencia, Spain.*

13 <sup>4</sup>*PhD, Associate Professor. Dipartimento Scienze Agrarie e Forestali (SAF), Università degli*  
14 *Studi, Viale delle Scienze 12, Palermo, Italy.*

## 15 16 **Abstract**

17 Agro-hydrological models are considered an economic and simple tool to quantify crop water  
18 requirements. In the last two decades, agro-hydrological physically based models have been  
19 developed to simulate mass and energy exchange processes in the soil-plant-atmosphere  
20 system. Although very reliable, due to the high number of required variables, simplified  
21 models have been proposed to quantify crop water consumes.

22 The main aim of the paper is to propose an amendment of FAO-56 spreadsheet program in  
23 order to introduce a more realistic shape of the stress function, valid for mature olive orchards  
24 (*Olea europaea* L.). The modified model is successively validated by means of the  
25 comparison between measured and simulated soil water contents and actual transpiration  
26 fluxes. These outputs are finally compared with those obtained with the original version of the  
27 model.

28 Experiments also allowed assessing the ability of simulated crop water stress coefficients to  
29 explain the actual water stress conditions evaluated on the basis of measured relative  
30 transpirations and midday stem water potentials.

31 The results show that the modified model significantly improves the estimation of actual crop  
32 transpiration fluxes and soil water contents under soil water deficit conditions, according to  
33 the RMSEs associated to the revised model, resulting significantly higher than the  
34 corresponding values obtained with the original version.

## 35 **Keywords**

36 FAO-56 agro-hydrological model, Water stress Function, Water uptake ability, Table Olive  
37 orchards. Midday Stem Water Potential, Relative Transpiration.

38

## 39 Introduction

40 The quantification of crop water requirements of irrigated land is crucial in the Mediterranean  
41 regions characterized by semi-arid conditions, where water scarcity and increasing  
42 competition for water resources are pressurizing farmers to adopt different water saving  
43 techniques and strategies, which may range from a simple periodic estimation of the soil  
44 water balance terms to a precise assessment of temporal and spatial distribution of water  
45 exchange within the soil–plant–atmosphere continuum (Provenzano et al., 2013).

46 The knowledge of actual transpiration fluxes can allow the correct estimation of crop water  
47 requirements and to dispose of irrigation management strategies aimed to increase water use  
48 efficiency. Physically based and stochastic hydrological models, although very reliable, in  
49 relation to the high number of variables and the complex computational analysis required  
50 (Laio et al., 2001, Agnese et al., 2013), cannot often be applied. The use of simplified models,  
51 considering a simple water bucket approach, may therefore represent a useful and simple tool  
52 for irrigation scheduling.

53 FAO Irrigation and Drainage Paper 56 (Allen et al., 1998) provides a comprehensive  
54 description of the widely accepted Penman-Monteith method to estimate reference  
55 evapotranspiration from standard weather data and also an affordable procedure to compute  
56 actual crop evapotranspiration under standard and non-standard (stressed) conditions. A first  
57 amendment of the algorithm, was recently proposed by Rallo et al. (2012) for arboreal crops  
58 in order to allow irrigation scheduling under soil water deficit conditions; with this  
59 modification the eco-physiological factor, affected by the crop stress, was separated from the  
60 Management Allowed Depletion (*MAD*) term, more related to the farmer choices and  
61 dependent on aleatory variables like the economic factors.

62 Even if several studies have been carried out (Fernández et al., 2001; Testi et al., 2004;  
63 Ezzahar et al., 2007; Er-Raki et al., 2008; Cammalleri et al, 2013) on the evaluation of olive  
64 water consumptions and in particular on the partition of the components of crop  
65 evapotranspiration in semiarid areas, a few studies have been considering the eco-  
66 physiological processes influencing the kinetic of root water uptake. This missing feature  
67 represents a limitation of the available version of the model that schematizes the crop water  
68 uptake by means of a transpiration reduction function in which the stress coefficient,  $K_s$ , is  
69 assumed linearly dependent on the soil water depletion, in the range between a certain critical  
70 value and the wilting point. Actually, the shape of  $K_s$  depends on eco-physiological processes,  
71 like plant resistance/tolerance/avoidance to water stress and soil water availability in the root  
72 zone. For xerophytes crops like olives, Rallo and Provenzano (2013) recognized a convex

73 shape of the  $K_s$  relationship and also that crop water stress conditions occur for soil matric  
74 potentials lower than -0.40 MPa. Moreover, it was showed that the reduction of actual  
75 transpiration becomes severe only under extreme water deficit conditions.

76 The main objective of the paper is to propose an amendment of FAO-56 original spreadsheet  
77 program and to assess its suitability to simulate table olive (*Olea europaea* L.) water  
78 requirement under soil water deficit conditions. In particular, a more realistic shape of the  
79 water stress function, valid for the considered crop, is introduced into the model in place of  
80 the original liner function; the validation is firstly carried out through the comparison between  
81 measured and simulated soil water contents (SWCs) and actual transpiration fluxes ( $T_a$ ).  
82 Outputs of the amended model are then compared with those obtained with the original  
83 version. Finally, the measured relative transpirations and midday stem water potentials  
84 ( $MSWP$ ) are used to evaluate the ability of simulated stress coefficients to explain the actual  
85 crop water stress conditions.

## 86 **Overview on FAO-56 dual approach model and critical analysis**

87 FAO 56 model evaluates the root zone depletion at a daily time step with a water balance  
88 model based on a simple tipping bucket approach:

$$89 \quad D_i = D_{i-1} - (P_i - RO_i) - I_i + ET_{c,i} + DP_i$$

90 (1)

91 where  $D_i$  [mm] and  $D_{i-1}$  [mm] are the root zone depletions at the end of day  $i$  and  $i-1$   
92 respectively,  $P_i$  (mm) is the precipitation,  $RO_i$  the surface runoff,  $ET_{c,i}$  [mm] is the actual  
93 evapotranspiration and  $DP_i$  [mm] is the deep percolation of water moving out of the root  
94 zone.

95 The domain of the depletion function,  $D_i$ , is between 0, which occurs when the soil is at the  
96 field capacity, and a maximum value, corresponding to the total plant available water,  $TAW$   
97 [mm], obtained as:

$$98 \quad TAW = 1000(SWC_{fc} - SWC_{wp})Z_r \quad (2)$$

99 where  $SWC_{fc}$  [ $\text{cm}^3 \text{cm}^{-3}$ ] and  $SWC_{wp}$  [ $\text{cm}^3 \text{cm}^{-3}$ ] are the soil water contents at field capacity  
100 and wilting point respectively and  $Z_r$  [m] is the depth of the root system.

101 In absence of water stress (potential condition), the crop potential evapotranspiration  $ET_c$  is  
102 obtained multiplying the dual crop coefficients ( $K_{cb} + K_e$ ) and the Penman-Monteith reference  
103 evapotranspiration rate,  $ET_0$ , (Allen et al., 1998). In particular the “dual crop coefficients  
104 approach”, as explained in FAO 56 paper, splits the single  $K_c$  factor in two separate terms, a

105 basal crop coefficient,  $K_{cb}$ , considering the plant transpiration and a soil evaporation  
 106 coefficient  $K_e$ .

107 When water represents a limiting condition, the basal crop coefficients,  $K_{cb}$ , has to be  
 108 multiplied to a reduction factor,  $K_s$ , variable between 0 and 1. The reduction factor can be  
 109 express by:

$$110 \quad K_s = \frac{TAW - D_i}{TAW - RAW} \quad (3)$$

111 where  $RAW$  [mm] is the readily available water, that can be obtained multiplying  $TAW$  to a  
 112 depletion coefficient,  $p$ , taking into account the resistance of crop to water stress. In  
 113 particular, when water stored in the root zone is lower than  $RAW$  ( $D_i > RAW$ ), the reduction  
 114 coefficient  $K_s$  is lower than 1, whereas for  $D_i \leq RAW$  results  $K_s=1$ . Values of  $p$ , valid for  
 115 different crops, are proposed in the original publication (Allen et al., 1998). Considering that  
 116 the term  $p$  depends of the atmospheric evaporative demand, a function for adjusting  $p$  for  $ET_c$   
 117 is suggested (van Diepen et al., 1988).

118 The soil evaporation coefficient,  $K_e$ , describes the evaporation component of  $ET_c$ . When the  
 119 topsoil is wet, i.e after a rainfall or an irrigation event,  $K_e$  is maximum. Drier the soil surface,  
 120 lower is  $K_e$ , with a value equal to zero when the water content of soil surface is equal to  
 121  $SWC_{wp}$ . When the topsoil dries out, less and less water is available for evaporation: the soil  
 122 evaporation reduction can be therefore considered proportional to the amount of water in the  
 123 soil top layer, or:

$$124 \quad K_e = MIN \left\{ \begin{array}{l} K_r * (K_{c\_max} - K_{cb}) \\ f_{ew} * K_{c\_max} \end{array} \right\} \quad (4)$$

125 where  $K_r$  is a dimensionless evaporation reduction coefficient depending on the cumulative  
 126 depth of water evaporated from the topsoil,  $f_{ew}$  is the fraction of the soil that is both exposed  
 127 and wetted, i.e. the fraction of soil surface from which most evaporation occurs and  $K_{c\_max}$  is  
 128 the maximum value of  $K_c$  following rain or irrigation;  $K_{c\_max}$  represents an upper limit of  
 129 evapotranspiration fluxes from any cropped surface, whereas the term  $f_{ew}$  depends on  
 130 vegetation fraction cover and irrigation system, the latter influencing the wetted area.

131 The evaporation decreases in proportion to the amount of water in the surface soil layer:

$$132 \quad K_r = \frac{TEW - D_{e,i-1}}{TEW - REW} \quad (5)$$

133 where  $D_{e,i-1}$  is cumulative depth of evaporation (depletion) from the soil surface layer at the  
134 end of (i-1)th day [mm],  $TEW$  [mm] is the total evaporable water from an effective depth  $Z_e$   
135 of soil surface subject to drying, and  $REW$  [mm] is the readily evaporable water, representing  
136 the maximum depth of water that can evaporate from the topsoil layer without restrictions.  
137 When  $TEW$  is unknown, it can be estimated as  $TEW = 1000(SWC_{fc} - 0.5SWC_{wp})Z_e$ , where  $Z_e$  is  
138 usually assumed equal to 0.10-0.15 m. On the other hand,  $REW$  can be estimated according to  
139 soil texture (Allen et al., 1998).

140 Buckets models are very sensitive to the rooting depth parameter,  $Z_r$ , directly influencing the  
141 ability of the plant to extract water. Errors in its determinations determine an incorrect  
142 estimation of soil water stress coefficient and, as indicated by Er-Raki et al. (2008), the values  
143 of simulated evapotranspiration increase with increasing  $Z_r$ . In fact, higher  $Z_r$  causes  
144 increments of  $TAW$  within the root zone and, according to eq. 3, leads to higher  $K_s$  values.

145

## 146 **Materials and methods**

147 Investigations were carried out during irrigation seasons 2009, 2010 and 2011 (from April 15,  
148 DOY 105 to September 30, DOY 273) in the experimental farm “Tenute Rocchetta”, located  
149 in Castelvetro (Sicily, UTM EST: 310050, NORD: 4168561). The farm, with an extension  
150 of about 13 ha, is mostly cultivated with table olive grove (*Olea europaea* L., var. Nocellara  
151 del Belice), representing the main crop in the surrounding area. The experimental plot is  
152 characterized by 17 years old olive trees, planted on a regular grid of 8 x 5 m (250 plants/ha);  
153 the mean canopy height is about 3.7 m and the average fraction of vegetation cover is about  
154 0.35. Irrigation is practiced by means of pipelines with on line emitters installed along the  
155 plant rows. Each plant was irrigated with four 8 l/h emitters. Soil textural class, according  
156 USDA classification, is silty clay loam.

157 Standard meteorological data (incoming short-wave solar radiation, air temperature, air  
158 humidity, wind speed and rainfall) were hourly collected by SIAS (Servizio Informativo  
159 Agrometeorologico Siciliano), with standard equipments installed about 500 m apart from the  
160 experimental field. Net radiation  $R$  and its components were measured with a 4-component  
161 net radiometer (NR01, Hukseflux). According to ASCE-ESRI, the standardized Penman-  
162 Monteith method (Allen et al., 2008) was used to calculate atmospheric water demand.

163 A preliminary investigation on the root spatial distribution was carried out in order to identify  
164 the soil volume within which the highest root density is localized and where most of water  
165 uptake processes occur. A more detailed description of the soil physical properties and the  
166 root distribution is presented and discussed in Rallo and Provenzano (2013).

167

168 Irrigation scheduling followed the ordinary management practised in the surrounding area.  
169 The total irrigation depth provided by the farmer was equal to 80 mm in 2009, 33 mm in 2010  
170 and 150 mm in the 2011.

### 171 **Soil and crop water status measurements**

172 During the investigation periods, soil water contents were measured with Time Domain  
173 Reflectometry (TDR 100, Campbell Inc.) and Frequency Domain Reflectometry (FDR,  
174 Diviner 2000, Sentek) probes. On the basis of the results of Rallo and Provenzano (2013), the  
175 soil volume in which most of the root absorption occurs have been considered, in order to  
176 install the soil moisture probes and to dispose of a representative measure of the average SWC  
177 in the entire system (Xiloyannis et al., 2012). In particular, the soil volume where 80% of  
178 roots are localized, can be assumed as a parallelepiped with a length equal to the tree spacing  
179 (5.0 m), a width of 1.5 m and a depth of 0.75 m. Referring to this soil volume, spatial and  
180 temporal variability of soil water contents was monitored, from the soil surface to a depth of  
181 100 cm, using a FDR probe. Five access tubes were installed along two parallel directions, the  
182 first below the irrigation pipeline, at distances of 1.0 m, 2.0 m and 2.5 m from the plant and  
183 the second along a parallel direction, at a distance of 0.50 m from the first and about 1.0 m  
184 and 2.50 m from the plant. In this way it was possible to take into account the spatial  
185 variability of soil water content after irrigation. Additional measurements of soil water  
186 contents were carried out using nine TDR probes connected to a multiplexer. The probes,  
187 having a length of 20 cm, were installed below the irrigation pipeline, at the same distances of  
188 the FDR access tubes, but opposite side of the plant, in the layer 10-30 cm, 35-55 cm and 60-  
189 80 cm. Values of soil water contents measured with FDR and TDR systems were then  
190 averaged in order to determine, for each measurement day, a single value of SWC  
191 representative of the soil layer where most of the root absorption takes place.

192 Transpiration fluxes were monitored on three consecutive trees, selected within the field  
193 according to their trunk diameter, so that they can be considered representative of the grove,  
194 using standard sap flow sensors (Thermal Dissipation Probes, Granier, 1987). For each plant,  
195 two probes were installed on the north side of the trunk and then insulated, to avoid the direct  
196 sun exposure. The measurements acquired by the two sensors were then averaged. The central  
197 plant was the same in which SWCs were measured.

198 Daily values of actual transpiration were obtained by integrating the sap flux, under the  
199 hypothesis to neglect the tree capacitance. Daily transpiration depth [ $\text{mm d}^{-1}$ ] was obtained  
200 dividing the daily flux [ $\text{l d}^{-1}$ ] for the pertinence area of the plant, equal to  $40 \text{ m}^2$ . Then, in

201 order to evaluate a representative value of the stand transpiration referred to the entire field, it  
 202 was necessary to up-scale the plant fluxes by considering, as a proximal variable, the ratio  
 203 between the average Leaf Area Index,  $LAI$  ( $m^2 m^{-2}$ ), measured in field, and the average value,  
 204  $LAI_p$  ( $m^2 m^{-2}$ ), measured on the plants in which sap fluxes were monitored.  
 205 In the same trees selected for transpiration measurements, midday stem water potentials  
 206 ( $MSWP$ ) were measured in 2009 and 2011 by using a pressure chamber (Scholander et al.,  
 207 1965), according to the protocol proposed by Turner e Jarvis (1982).

## 208 **Amendment of the FAO-56 model and parameterization of soil and crop**

209 FAO 56 model has been applied i) in the original form and ii) in its amended version, in  
 210 which the stress function, the threshold value of the soil water content below which water  
 211 stress occurs,  $SWC^*$ , and the minimum seasonal value of soil water content recognized in the  
 212 field,  $SWC_{min}$ , were experimentally determined.

213 In the first case, the model parameter  $p$  was assumed equal to 0.65, as indicated in table 22 of  
 214 the original paper, corresponding for the investigated soil to  $SWC^*=0.20$ , whereas  $SWC_{fc}$  and  
 215  $SWC_{wp}$  were considered equal to 0.33 and 0.13, determined according to the soil water  
 216 retention curve, for matric potentials of -0.33 MPa and -1.50 MPa respectively.

217 In the second case, in order to consider a more realistic water stress response of olive crops,  
 218 the original function, as implemented in the model, was modified according to the  
 219 relationship proposed by Steduto et al., 2009, in which  $K_s$  is a function of the relative  
 220 depletion,  $D_{rel}$ :

$$221 \quad K_s = 1 - \frac{e^{D_{rel} f_s} - 1}{e^{f_s} - 1} \quad (6)$$

222 where  $f_s$  is a fitting parameter characterizing the shape of the stress function. The value of  $f_s$   
 223 was assumed equal to 2.89 as experimentally determined by Rallo and Provenzano (2013).

224 Relative depletion can be determined as:

$$225 \quad D_{rel} = \frac{SWC^* - SWC}{SWC^* - SWC_{min}} \quad (7)$$

226 in the domain of soil water contents determining stress conditions for the crop  
 227 ( $SWC_{min} < SWC < SWC^*$ ).

228 Fig. 1 shows the water stress function, as implemented in the spreadsheet program.

229  
 230  
 231  
 232  
 233

**Figure 1 – Water stress functions for table olive orchards, as implemented in the spreadsheet**

234 The shape of the considered function evidences that the water stress models is convex and  
235 demonstrates that water stress becomes more and more severe at decreasing soil water status  
236 ( $D_{rel}$  tending to 1); therefore, the reduction of actual transpiration is critical only for the most  
237 extreme water stress conditions. Moreover, the modified crop water stress function allows  
238 smoothing the unrealistic angular point indicating, in the  $K_s$  linear relationship, the passage  
239 from no-water stress to water stress conditions.

240 Under the investigated conditions,  $SWC^*$  and  $SWC_{min}$  was assumed to correspond to a matric  
241 potential of -0.4 MPa representing the thresholds soil water status separating a condition of  
242 negligible water stress (relative transpiration is approximately equal to 1) from a condition in  
243 which relative transpiration decreases with soil water content (Rallo and Provenzano, 2013).

244 On the other side,  $SWC_{min}=0.07 \text{ m}^3 \text{ m}^{-3}$ , lower than the measured wilting point of  $0.13 \text{ m}^3 \text{ m}^{-3}$ ,  
245 represents the minimum soil water content measured during the investigated seasons. The  
246 choice to consider  $SWC_{min}$  as the minimum seasonal value of soil water content recognized in  
247 the field and not the soil wilting point, as traditionally used for most crops, followed the  
248 suggestion of Ratliff et al., 1983 and, more recently, of Pellegrino et al. (2006). This  
249 assumption allowed to consider the strong ability of olive trees to extract water from the soil  
250 even below the soil wilting point and consequently a more coherent evaluation of the crop  
251 water availability (Lacape et al., 1998).

252 The depth of the root system,  $Z_r$ , was assumed equal to 0.75 m, as obtained on the basis of the  
253 measured root distribution, corresponding to the soil layer within which 80% of roots were  
254 encountered (Martin et al., 1999).

255 The average value of basal crop coefficient, in the mid and late stage seasons, was considered  
256 equal to 0.60, as recommended from Allen et al. (1998) and recently verified in the same  
257 experimental field (Minacapilli et al., 2009; Cammalleri et al., 2013).

258 Simulations were run during the three investigated years, from DOY 105 to DOY 273. For all  
259 the investigated periods,  $SWC_{fc}$  equal to  $0.33 \text{ m}^3 \text{ m}^{-3}$  was considered as initial condition, as a  
260 consequence of the copious precipitation occurred in the decade antecedent mid of April each  
261 year.

262 The values of the simulations variables, used as input for the original and modified models,  
263 are showed in Tables 1.

264

265 **Tab. 1 –Values of the variables used for the simulations carried out with the original and**  
266 **modified FAO 56 model.**

267



## 268 Performance of the models

269 The performance of the models was evaluated by the root mean square error (RMSE), and the  
270 mean bias error (MBE), defined as:

$$271 \quad RMSE = \sqrt{\left(\frac{1}{N} \sum_{i=1}^N d_i^2\right)} \quad (8)$$

$$272 \quad MBE = \frac{1}{N} \sum_{i=1}^N d_i \quad (9)$$

273 where  $N$  is the number of measured data,  $d_i$  is the difference between predicted and measured  
274 values (Kennedy and Neville, 1986).

275 An additional Student t-test was applied, as proposed by Kennedy and Neville (1986):

$$276 \quad t = \sqrt{\frac{(N-1)MBE^2}{RMSE^2 - MBE^2}} \quad (10)$$

277 To determine if the differences between measured and simulated soil water contents are  
278 statistically significant, the absolute value of the calculated  $t$  must be less than the critical  $t$   
279 value ( $t_{crit}$ ), for a fixed significance level. In this analysis, a significance level  $\alpha=0.05$  was  
280 assumed.

281

## 282 Results and discussion

283 Fig. 2 shows the temporal dynamic of measured  $SWCs$  during the investigation periods 2009,  
284 2010 and 2011 (2a-c), as well as the estimated potential crop transpiration (dashed line),  $T_c$ ,  
285 and the measured actual transpiration,  $T_a$ , in the same time intervals (2d-f). In addition the  
286 figure displays the corresponding simulation results obtained by considering the original  
287 (light line) and the modified (bold line) versions of the model. At the top of the figure the  
288 water supplies (precipitation and irrigation) are also shown.

289 As can be observed, compared to the original version, the amended model, provides better  
290 estimation in terms of either actual transpiration fluxes and soil water contents.

291 The statistical comparison, express in term of  $RMSE$  and  $MBE$  associated to  $SWC$  and  $T_a$   
292 simulated by modified and original models are presented in table 2.

293

294 **Fig. 2a-i - Temporal dynamic of observed and simulated  $SWCs$  and  $T_a$  fluxes during**  
295 **2009, 2010 and 2011. Potential transpiration fluxes and total water supplies are also**  
296 **shown**

297

298

299 **Tab. 2 – *RMSEs* and *MBEs* associated to *SWC* and actual  $T_a$  simulated with the**  
300 **original and modified models**  
301

302 A substantial agreement between measured average soil water contents in the root zone and  
303 the corresponding values, simulated with the revised model, is generally observed, with a root  
304 mean square error variable between 0.03 and 0.09.

305 Moreover, after a first simulation period in which the results of original and amended models  
306 are identical (absence of crop water stress), the original model determines a systematic  
307 overestimation of *SWC*, with *RMSE* variable between 0.05 and 0.10. The better estimation of  
308 minimum values of *SWC* obtained with the modified model is a consequence of considering  
309  $SWC_{min}$  in place of  $SWC_{wp}$ , allowing a better modeling of the root water uptake ability, as  
310 actually recognized for olive trees.

311 As can be observed in fig. 2d-f, the seasonal trends of actual daily transpiration fluxes  
312 simulated with the modified model, in all the investigated periods, generally follow the  
313 observed values with *RMSE*, on average, equal to 0.54 mm if considering all the data. Despite  
314 the reasonable global agreement, some local discrepancies can be observed in the periods  
315 immediately following irrigations (wetting events) in which peak values of  $T_a$ , due to the  
316 quick decrease of the depletion, are simulated. This evidence is corroborated by Liu and Luo  
317 (2010) and Peng et al. (2007), who observed that the dual approach of FAO-56 is appropriate  
318 for simulating the total quantity of evapotranspiration, but inaccurate in simulating the peak  
319 values after precipitation or irrigation.

320 The highest differences between simulated (modified model) and measured actual  
321 transpiration fluxes, observed from mid of July and end of August 2010 ( $RMSE=0.78$  mm),  
322 could be due to the neglected contribute to transpiration of the water stored in the tree. After  
323 any input of water in the soil, in fact, even the modified model does not consider the water  
324 redistribution processes occurring in the soil, as well as the tree capacitance effect, taking into  
325 account the increasing water stored in the leaves, branches and trunk of the tree. Anyway,  
326 contribution of the tree capacitance on transpiration fluxes needs a more specific  
327 investigation, in order to further improve the FAO-56 model framework. In addition, the  
328 result could be also due to the circumstance that after a prolonged drought period, it is  
329 possible that trees activate the portion of the root system placed outside the soil volume where  
330 soil moisture was actually monitored.

331 On the other hands, if comparing the original and the revised version of the model  
332 characterized of average *RMSE* values (all the data) equal to 1.40 mm and 0.54 mm  
333 respectively (table 2), it is evident that for both the simulations the predicted transpiration  
334 fluxes are coincident during the first period of simulation (absence of crop water stress) and

335 become quite different in the subsequent dry periods (fig. 2). The quickest reductions of  
336 actual transpiration fluxes, visible for the original model, are a direct consequence of the  
337 adopted linear stress function, detecting a rapid reduction of the  $K_s$  coefficient since the initial  
338 phase of the crop water stress.

339 Moreover, during dry periods, despite simulated  $SWC_s$  were generally higher than the  
340 corresponding measured, the values of actual transpiration resulted systematically lower.

341 Table 3 shows the statistical comparison in terms of Student-t test. As can be observed,  
342 differences between measured  $SWC$  and  $T_a$  values and the corresponding estimated by the  
343 revised model are statistically not significant ( $\alpha=0.05$ ) in 2009 and 2011, while they are  
344 always significantly different when the original model is considered. According to this result,  
345 it is evident that the modified model considerably improves the estimation of soil water  
346 content and actual transpiration fluxes.

347

348 **Tab. 3 – Student-t related to  $T_a$  and  $SWC$  obtained with the original and modified**  
349 **model. The corresponding critical t-values are also shown**

350

351 Fig. 3a-c shows, from the beginning of July to the end of September each year, the  
352 comparison between actual measured cumulative transpiration fluxes together with the  
353 corresponding predicted by the original (light line) and amended (bold line) version of the  
354 model. As discussed, except that for a certain underestimation observable since the end of  
355 July 2010, compared to the original model, the modified version estimates quite well the  
356 cumulative crop water consumes during the examined periods.

357

358 **Fig. 3a-c - Comparison between cumulative tree transpiration fluxes simulated by**  
359 **the models for a) 2009, b) 2010 and c) 2011 seasons and corresponding measured**  
360 **values (white circles)**

361

362 The better performance of simulated transpiration fluxes obtained with the modified model is  
363 therefore consistent with the combined effects of the improved  $SWC$  estimation and the more  
364 adequate schematization of the stress function.

365 Additional simulations evidenced that, assuming the depletion fraction  $p$ , as computed on the  
366 basis of experimental  $SWC^*$  and  $SWC_{min}$ , without modifying the stress function, slightly  
367 improve the estimation of soil water contents and actual transpiration fluxes compared to the  
368 original version of the model (data not showed), due to the increased total available water and  
369 to the reduced slope of the stress function. This results indicated that the impact on simulated  
370 variables ( $SWC$  and  $T_a$ ) is mainly due to the shape of the stress function, more than the choice  
371 of  $SWC^*$  and  $SWC_{min}$ .

372 In order to assess the ability of simulated crop water stress coefficient to explain the actual  
373 water stress conditions, fig. 4a-c shows the temporal dynamic of measured relative  
374 transpirations and simulated  $K_s$  values obtained with the original (light line) and modified  
375 (bold line) model. Midday stem water potentials are also shown in the secondary axis,  
376 whereas total water supplies are presented at the top of the figure.

377

378 **Fig. 4a-f - Temporal dynamic of measured relative transpiration,  $T_a T_c^{-1}$ , and**  
379 **simulated water stress coefficient,  $K_s$ , during 2009, 2010 and 2011. Measured**  
380 **midday stem water potential (MSWP) and total water supply are also shown**  
381

382 As can be observed, both the models determines a quick increasing of the relative  
383 transpiration immediately after irrigations, similarly to what observed for actual transpiration.  
384 Even in this case the modified model allows to better explain the dynamic of relative  
385 transpiration, showing a convex curve reflecting the marked tendency of the  $K_s$ (SWC)  
386 relationship. Conversely, the stress coefficient simulated by the original model systematically  
387 underestimates the relative transpiration with an opposite tendency, certainly due to the  
388 misrepresentation of the stress function. Additionally, if the amended model allows  
389 determining  $K_s$  values not lower than 0.6, as observed in the field in terms of relative  
390 transpiration, with the unmodified model unrealistic lower  $K_s$  are displayed, with a minimum  
391 of about 0.1. In the same figure it can be evidenced that the water stress coefficients follow  
392 the general seasonal trend observed for midday stem water potentials.

393 Fig. 5a-b illustrates the predicted  $K_s$  values, as a function of *MSWPs*, respectively obtained  
394 when the original and the modified model are considered. The regression equations,  
395 characterized by  $R^2=0.06$  and 0.46 respectively, are also shown. As can be observed in the  
396 figure,  $K_s$  values estimated with the modified model are characterized by a lower variability  
397 compared to those evaluated with the original FAO 56 model; furthermore, for the revised  
398 model, the fitted regression allows to explain the variance of the considered *MSWP* data set.

399

400 **Fig. 5a-b - Relationships between water stress coefficient,  $K_s$ , and midday stem**  
401 **water potential, *MSWP*, in the original (left) and modified (right) FAO 56 model**  
402

403 This result is well in agreement to the relationship experimentally obtained in 2008 using  
404 independent measurements of relative transpiration and midday stem water potential  
405 (unpublished data) and evidences how the modified model is able to properly reproduce, for  
406 the investigated crop, the stress conditions as recognized in the field.

407

## 408 **Conclusions**

409 In the paper, an improvement of FAO 56 spreadsheet program, aimed to consider a more  
410 realistic convex shape of the stress function for drought tolerant crops like olive trees, has  
411 been proposed and assessed.

412 The suitability of the amended agro-hydrological model was verified according to soil water  
413 contents and actual transpiration fluxes measured during the three irrigation seasons 2009,  
414 2010 and 2011. At the same time, the ability of the model to simulate crop water stress  
415 coefficients was also verified on the basis of an independent dataset of midday stem water  
416 potentials measured in the field.

417 Compared to the original version, the modified model allows a better modelling of the root  
418 water uptake ability and consequently to predict quite well the soil water contents in the root  
419 zone, with differences generally not statistically significant ( $\alpha=0.05$ ). In fact, the assumption  
420 of the minimum soil water content measured in the field, in place of the traditionally used  
421 wilting point, allowed taking into account the root ability of olive trees to extract water from  
422 the soil.

423 The amendment of the original model also permitted a considerable enhancement in the  
424 estimation of actual transpiration fluxes, as confirmed by the Student-t test applied for the  
425 three investigated seasons. The better performance of simulated fluxes is consistent firstly  
426 with the combined effects of the more realistic schematization of the stress function and  
427 secondly with the improved estimation of soil water content thresholds.

428 The underestimation of actual transpiration fluxes observed in the period from mid of July to  
429 the end of August 2010 could be due to the soil volume explored by the roots and/or to the  
430 neglected contribute of the tree capacitance, related to the water stored in the leaves, branches  
431 and trunk of the tree. This aspect needs a more specific investigation in order to verify the  
432 possibility of a further improvement of FAO-56 model.

## 433 **Acknowledgements**

434 A special thanks to Dr. Pierluigi Crescimanno, manager of the farm “Tenute Rocchetta”  
435 hosting the experiments, for his great sensibility to any subject related to environmental  
436 safeguard.

437 Research was carried out in the frame of the projects PRIN 2010 co-financed by Ministero  
438 dell'Istruzione, dell'Università e della Ricerca (MIUR) and FFR 2012-2013 granted by  
439 Università degli Studi di Palermo.

440 The contribution to the manuscript has to be shared between authors as following:  
441 Experimental set-up, data processing and final revision of the text have to be divided equally  
442 between Authors. Field data collection was cared by G. Rallo. Text was written by G. Rallo  
443 and G. Provenzano.

444

## 445 **References**

446 Agnese, C., Baiamonte, G., Cammalleri, C. (2013), “ Probabilistic modelling of the occurrence  
447 of rainy days”. Submitted to *Advances in Water Research*.

448

449 Allen, R.G., Periera, L.S., Raes, D., Smith, M. (1998). *Crop Evapotranspiration: Guidelines*  
450 *for Computing Crop Requirements, Irrigation and Drainage Paper No. 56*. FAO, Rome, Italy,  
451 pp. 300.

452

453 Cammalleri, C., Rallo, G., Agnese, C., Ciralo G., Minacapilli, M., Provenzano, G. (2013).  
454 Combined use of eddy covariance and sap flow techniques for partition of ET fluxes and  
455 water stress assessment in an irrigated olive orchard. *Agric. Water Manage.* 120, 89-97.

456

457 Er-Raki, S., Chehbouni, A., Hoedjes, J., Ezzahar, J., Duchemin, B., Jacob, F. (2008).  
458 Improvement of FAO-56 method for olive orchards through sequential assimilation of  
459 thermal infrared based estimates of ET. *Agric. Water Manage.* 95, 309–321.

460

461 Ezzahar, J., Chehbouni, A., Hoedjes, J.C.B., Er-Raki, S., Chehbouni, Ah., Bonnefond, J.- M.,  
462 De Bruin, H.A.R. (2007). The use of the scintillation technique for estimating and monitoring  
463 water consumption of olive orchards in a semi-arid region. *Agric. Water Manage.* 89, 173–  
464 184.

465

466 Fernández, J.E., Palomo, M.J., Díaz-Espejo, A., Clothier, B.E., Green, S.R., Giron, I.F.,  
467 Moreno, F. (2001). Heat-pulse measurements of sap flow in olives for automating irrigation:  
468 tests, root flow and diagnostics of water stress. *Agric. Water Manage.* 51, 99–123.

469

470 Granier A (1987) Mesure du flux de seve brute dans le tronc du Douglas par une nouvelle  
471 methode thermique. *Ann. Sci. For.* 44:1-14.

472

473 Kennedy, J.B., Neville, A.M. (1986). *Basic Statistical Methods for Engineers and Scientists*.  
474 3rd edn. Harper & Row, New York.

475

476 Lacape, M.J., Wery, J., Annerose, D.J.M. (1998). Relationships between plant and soil water  
477 status in five field-grown cotton (*Gossypium hirsutum* L.) cultivars. *Field Crop Res.* 57, 29–  
478 43.

479

480 Laio, F., Porporato, A., Ridolfi, L., Rodriguez-Iturbe, I. (2001), Plants in water-controlled  
481 ecosystems: active role in hydrologic processes and response to water stress II. Probabilistic  
482 soil moisture dynamics, *Adv. Water Resour.*, 24(7), 707-723, doi:10.1016/S0309-  
483 1708(01)00005-7.

484

485 Liu, Y., Luo, Y. (2010). A consolidated evaluation of the FAO-56 dual crop coefficient  
486 approach using the lysimeter data in the North China Plain. *Agric. Water Manage.* 97, 31–40.

487  
488 Martin, C.D., Moffat, A.J. (1999). Examination of tree and root performance on closed  
489 landfills in Merseyside. *Arbor. J.* 23(3), 261-272. doi:10.1080/03071375.1999.9747244  
490  
491 Minacapilli, M., Agnese, C., Blanda, F., Cammalleri, C. , Ciraolo, G., D'Urso, G., Iovino, M.,  
492 Pumo, D., Provenzano, G., Rallo, G. (2009). Estimation of Mediterranean crops  
493 evapotranspiration by means of remote-sensing based models. *Hydr. and Earth Syst. Scie.* 13,  
494 1061-1074.  
495  
496 Pellegrino A., Goz' e, E., Lebon, E., Wery, J. (2006). A model-based diagnosis tool to  
497 evaluate the water stress experienced by grapevine in field sites. *Europ. J. Agron.* 25, 49–59.  
498  
499 Peng, S., Ding, J., Mao, Z., Xu, Z., Li, D. (2007). Estimation and verification of crop  
500 coefficient for water saving irrigation of late rice using the FAO-56 method. *Trans. CSAE* 23  
501 (7), 30–34.  
502  
503 Provenzano, G., Tarquis, A.M., Rodriguez-Sinobas, L. (2013). Soil and irrigation  
504 sustainability practices. *Agric. Water Manage.* 120, 1-4.  
505  
506 Rallo, G., Agnese, C., Minacapilli, M., Provenzano, G. (2012). Comparison of SWAP and  
507 FAO agro-hydrological models to schedule irrigation of wine grape. *J. Irr. and Drain. Eng.*  
508 138(7), 581–591.  
509  
510 Rallo, G., Provenzano, G. (2013). Modelling eco-physiological response of table olive trees  
511 (*Olea europaea* L.) to soil water deficit conditions. *Agric. Water Manage.* 120, 79-88.  
512  
513 Ratliff, L.F., Ritchie, J.T., Cassel, D.K. (1983). Field-measured limits of soil water  
514 availability as related to laboratory-measured properties. *Soil Sci. Soc. Am. J.* 47, 770–775.  
515  
516 Scholander, R.R., Hammel, H.T., Bradstreet, E.D., Hemmielsen, E.A. (1965). Sap pressure in  
517 16 vascular plants. *Science.* 148, 339-346.  
518  
519 Steduto, P., Hsiao, T.C., Raes, D., Fereres, E. (2009). AquaCrop. The FAO crop model to  
520 simulate yield response to water. Reference Manual.  
521  
522 Testi, L., Villalobos, F.J., Orgaz, F. (2004). Evapotranspiration of a young irrigated olive  
523 orchard in southern Spain. *Agric. For. Meteorol.* 12, 1–18.  
524  
525 Turner, M.T., Jarvis, G.P. (1982). Measurement of plant water status by the pressure chamber  
526 technique. *Irrig. Sci.* 9, 289-308.  
527  
528 Van Diepen, C. A., Rappoldt, C., Wolf, J., van Keulen, H. (1988). CWFS crop growth  
529 simulation model WOFOST. Documentation; Version 4.1, Centre for World Food Studies,  
530 Wageningen, The Netherlands.  
531  
532 Xiloyannis C., Montanaro, G., Dichio, B. (2012). Irrigation in Mediterranean fruit tree  
533 orchards. Irrigation systems and practices in challenging environments: edited by Teang Shui  
Lee INTECH 2012.

**Tab. 1 –Values of the variables used for the simulations carried out with the original and modified FAO 56 model.**

Variables	Original model			Modified model		
	2009	2010	2011	2009	2010	2011
Soil water content at field capacity, $SWC_{fc}$ [ $m^3/m^3$ ]	0.33	0.33	0.33	0.33	0.33	0.33
Soil water content at wilting point, $SWC_{wp}$ [ $m^3/m^3$ ]	0.13	0.13	0.13	n.u	n.u	n.u
Minimum soil water content, $SWC_{min}$ [ $m^3/m^3$ ]	n.u	n.u	n.u	0.07	0.07	0.07
Total Available Water, $TAW$ [mm]	150	150	150	n.u	n.u	n.u
Depletion factor, $p$ [%]	65	65	65	n.u	n.u	n.u
Total Evaporable Water, $TEW$ [mm]	22.5	22.5	22.5	22.5	22.5	22.5
Readily Evaporable Water, $REW$ [mm]	11.0	11.0	11.0	11.0	11.0	11.0
Fraction of soil surface wetted by irrigation, $f_w$ [-]	0.11	0.11	0.11	0.11	0.11	0.11
Number of day of the year at time of planting, $J_{plant}$ [-]	105	105	105	105	105	105
Number of day of the year at beginning of development period, $J_{dev}$ [-]	135	135	135	135	135	135
Number of day of the year at beginning of midseason period, $J_{mid}$ [-]	225	225	225	225	225	225
Number of day of the year at beginning of late season period, $J_{late}$ [-]	285	285	285	285	285	285
Number of day of the year at time of harvest or death, $J_{harv}$ [-]	375	375	375	375	375	375
Basal crop coefficient at initial season, $K_{cb\ ini}$ [-]	0.55	0.55	0.55	0.55	0.55	0.55
Basal crop coefficient at mid-season, $K_{cb\ mid}$ [-]	0.60	0.60	0.60	0.60	0.60	0.60
Basal crop coefficient at late-season, $K_{cb\ end}$ [-]	0.60	0.60	0.60	0.60	0.60	0.60
Maximum crop height, $H$ [m]	3.0	3.0	3.0	3.0	3.0	3.0
Minimum rooting depth, $Z_r$ [m]	0.75	0.75	0.75	0.75	0.75	0.75
Maximum rooting depth, $Z_r$ [m]	0.75	0.75	0.75	0.75	0.75	0.75
Midseason, Average, Wind Speed [ $m\ s^{-1}$ ]	0.99	1.34	1.38	0.99	1.34	13.8
Midseason, Average, $RH_{min}$ [%]	52.6	52.2	53.1	52.6	52.2	53.1

n.u.= not used in the simulations



**Tab. 2 – RMSEs and MBEs associated to soil water contents and actual transpiration fluxes simulated with the modified and original models**

	Year	Number of data (N)			Root Mean Square Error (RMSE)			Mean Bias Error (MBE)		
		Actual Transp.	FDR SWC	TDR SWC	Actual Transp.	FDR SWC	TDR SWC	Actual Transp.	FDR SWC	TDR SWC
		[-]	[-]	[-]	[mm]	[cm <sup>3</sup> cm <sup>-3</sup> ]	[cm <sup>3</sup> cm <sup>-3</sup> ]	[mm]	[cm <sup>3</sup> cm <sup>-3</sup> ]	[cm <sup>3</sup> cm <sup>-3</sup> ]
<b>ORIGINAL</b>	<b>all data</b>	381	43	337	1.02	0.06	0.08	0.64	-0.03	-0.04
	<b>2009</b>	104	16	80	1.06	0.05	0.06	0.68	-0.03	-0.04
	<b>2010</b>	125	11	118	1.25	0.04	0.06	0.93	-0.03	-0.05
	<b>2011</b>	152	16	139	0.75	0.08	0.10	0.37	-0.04	-0.03
<b>MODIFIED</b>	<b>all data</b>	381	43	337	0.54	0.06	0.07	-0.14	-0.02	0.00
	<b>2009</b>	104	16	80	0.44	0.04	0.04	-0.08	-0.01	0.01
	<b>2010</b>	125	11	118	0.78	0.05	0.03	-0.37	-0.04	0.00
	<b>2011</b>	152	16	139	0.30	0.07	0.09	0.01	-0.01	-0.01

**Tab. 3 – Student-t related to  $T_a$  and SWC obtained with the modified and original model. The corresponding critical  $t$ -values are also shown**

	Year	Number of data (N)			Actual Transp.		FDR SWC		TDR SWC	
		$T_a$	FDR SWC	TDR SWC	Student $t$	$t_{crit}$ ( $\alpha=0.05$ )	Student $t$	$t_{crit}$ ( $\alpha=0.05$ )	Student $t$	$t_{crit}$ ( $\alpha=0.05$ )
<b>ORIGINAL</b>	<b>all data</b>	381	43	337	15.57	1.97	4.12	2.02	11.94	1.97
	<b>2009</b>	104	16	80	8.49	1.98	2.64	2.13	11.98	1.99
	<b>2010</b>	125	11	118	12.4	1.98	3	2.23	21.38	1.98
	<b>2011</b>	152	16	139	6.91	1.98	2.29	2.13	3.89	1.98
<b>MODIFIED</b>	<b>all data</b>	381	43	337	5.15	1.97	1.92	2.02	0.29	1.97
	<b>2009</b>	104	16	80	1.81	1.98	0.96	2.13	1.72	1.99
	<b>2010</b>	125	11	118	6.02	1.98	3.66	2.23	0.63	1.98
	<b>2011</b>	152	16	139	0.53	1.98	0.36	2.13	0.7	1.98

Figure 1

[Click here to download Figure: FIG-1.pdf](#)

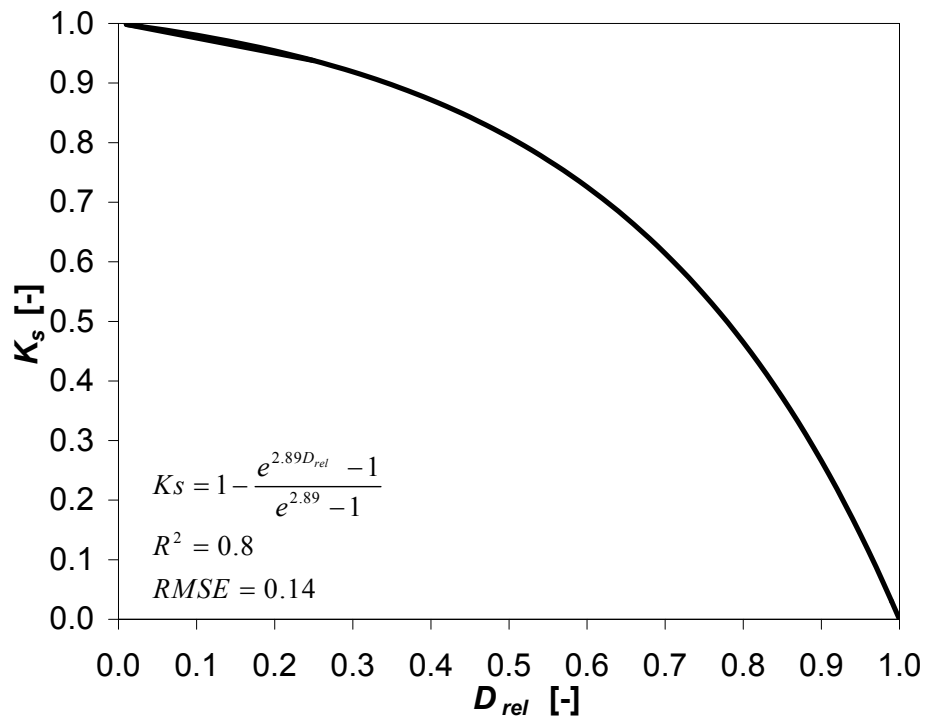


Figure 2

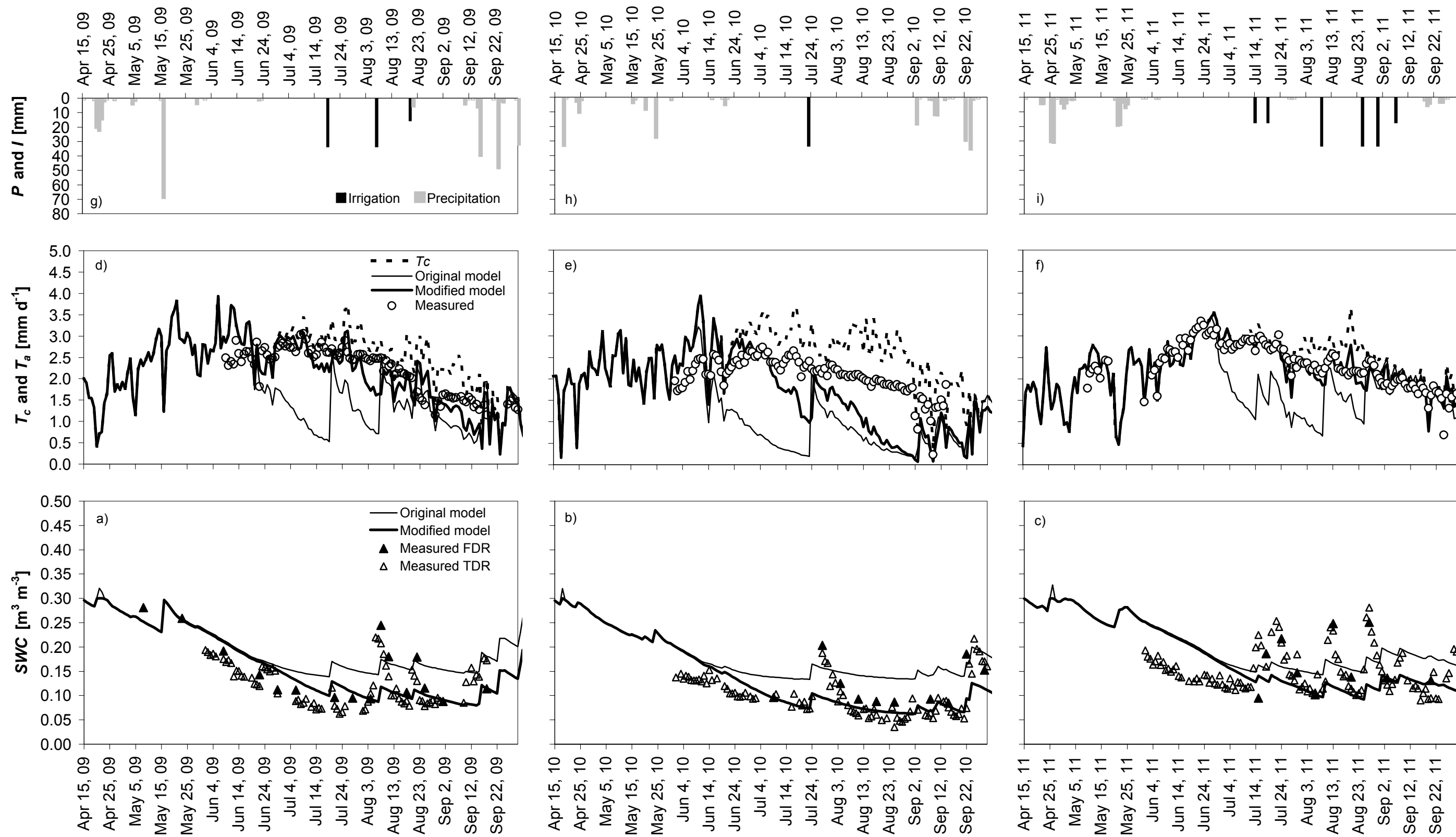
[Click here to download Figure: FIG-2.pdf](#)

Figure 3  
[Click here to download Figure: FIG-3.pdf](#)

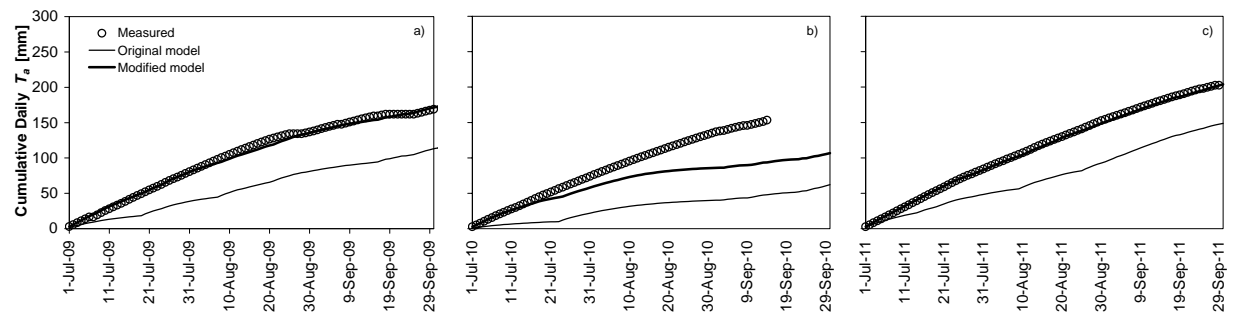


Figure 4

[Click here to download Figure: FIG-4.pdf](#)

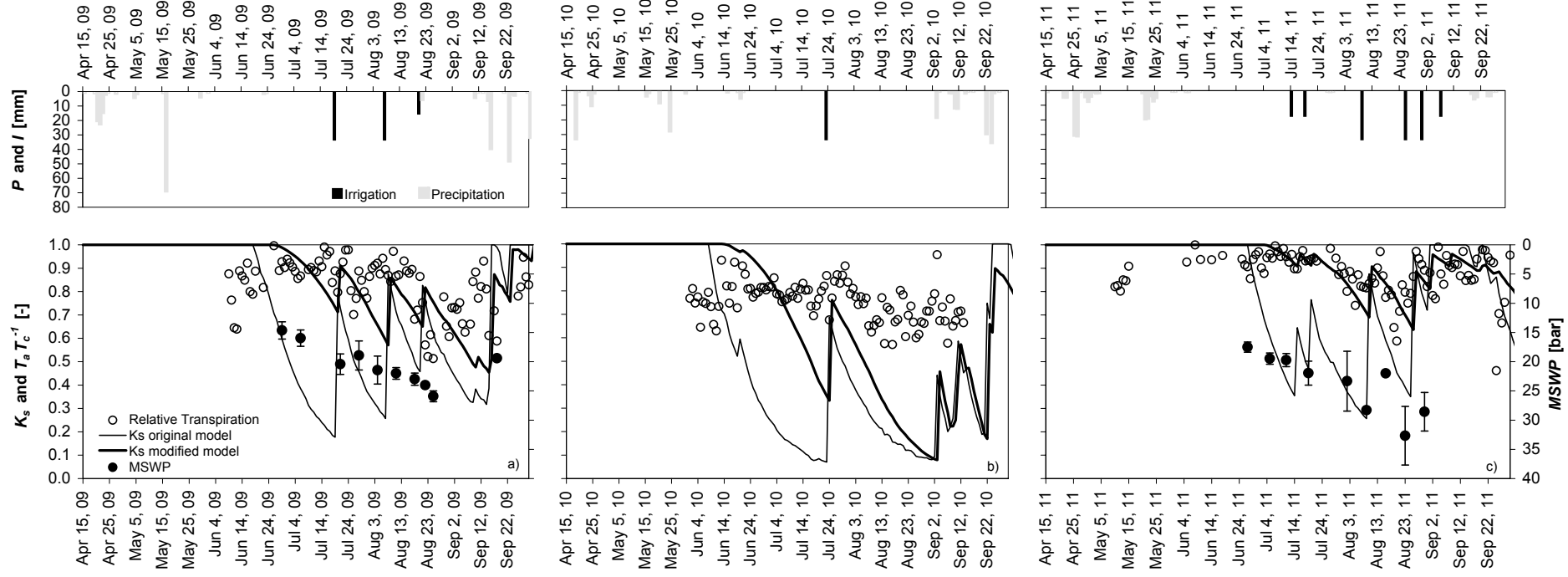
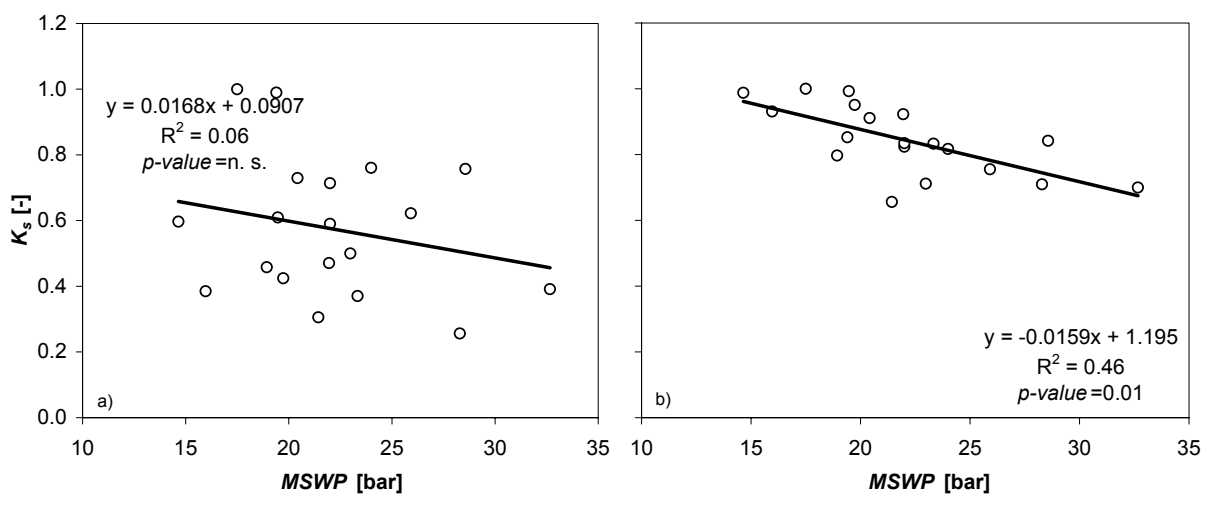


Figure 5  
[Click here to download Figure: FIG-5.pdf](#)



## Figure Caption List

Fig. 1 – Water stress functions for table olive orchards, as implemented in the spreadsheet

Fig. 2a-i - Temporal dynamic of observed and simulated soil water content and actual transpiration fluxes during 2009, 2010 and 2011. Potential transpiration and total water supplies are also shown

Fig. 3a-c - Comparison between cumulative tree transpiration fluxes simulated by the models for a) 2009, b) 2010 and c) 2011 seasons and corresponding measured values (white circles)

Fig. 4a-f - Temporal dynamic of measured relative transpiration,  $T_a T_c^{-1}$ , and simulated water stress coefficient,  $K_s$ , during 2009, 2010 and 2011. Measured midday stem water potentials (*MSWP*) and total water supplies are also shown

Fig. 5a-b - Relationships between water stress coefficient,  $K_s$ , and midday stem water potential, *MSWP*, in the original (left) and modified (right) model